Quick-and-Dirty Computation of Voigt Profiles, Classification of Their Shapes, and Effective Determination of the Shape Parameter

Achim Kehrein[1] and Oliver Lischtschenko[2]

[1] Rhine-Waal University of Applied Sciences,
Marie-Curie Str. 1, 47533 Kleve, Germany
[2] Ocean Insight - A Brand of Ocean Optics B.V.,
Maybachstr. 11, 73760 Ostfildern, Germany

Abstract A spectral line is modeled by a Voigt profile, which is a convolution of a Gaussian and a Lorentzian. The width of the Gaussian is described by the standard deviation σ; the width of the Lorentzian, by its lower quartile γ. One common method of computing a Voigt profile uses the real part of the complex-valued Faddeeva function, which is conceptually demanding and whose evaluation is computationally expensive. Other computational methods approximate Voigt profiles by simpler functions. We show that the shape of a Voigt profile only depends on the ratio $\rho = \gamma/\sigma$ and, consequently, introduce a one-parameter family of standardized Voigt profiles. Then we present a conceptually simple and efficient numerical method for computing these standardized Voigt profiles – we only require basic numerical integration. Next we compute the second derivative by a finite-difference formula and determine empirically the relationship between the shape parameter ρ and the location of the inflection points described by their quantiles. This empirical relationship suffices to determine the parameters of a Voigt profile directly from data points and thus avoids the use of computationally costly, time-consuming, and sometimes failing general iterative fitting methods. In particular, this new and faster approach allows more real-time analyses of spectral data.

Keywords Voigt profile, classification, standardization, computation, line spectra analysis, spectroscopy

1 Introduction

The centered Voigt profile is defined as the convolution

$$V(x;\sigma,\gamma) = \int_{-\infty}^{+\infty} G(x-z;\sigma)L(z;\gamma)\,dz \tag{1}$$

of a centered Gaussian and a centered Lorentzian,

$$G(x;\sigma) = \frac{1}{\sigma\sqrt{2\pi}}e^{-\frac{x^2}{2\sigma^2}} \quad \text{and} \quad L(x;\gamma) = \frac{\gamma}{\pi(x^2+\gamma^2)} \tag{2}$$

with width parameters $\sigma > 0$ and $\gamma > 0$. For any pair of parameters, the total area of the Voigt profile is one,

$$\int_{-\infty}^{\infty} V(x;\sigma,\gamma)\,dx = 1 \quad . \tag{3}$$

Thompson reviews some computational algorithms [1]. Based on work by Johnson, Wuttke provides a library in which the Voigt profile is computed via the complex Faddeeva function [2].

Section 2 briefly reviews the geometries of the Gaussian and the Lorentzian. The section particularly stresses that up to scaling and shifting there is only one shape of a Gaussian - the standardized Gaussian is the shape prototype. Moreover, the inflection point of the Gaussian reveals the width parameter. Section 3 shows that the shape of a Voigt profile depends only on the ratio of the parameters $\rho = \gamma/\sigma$. Therefore Voigt profiles form a one-parameter family of the standardized form $V(x;1;\rho)$ with *shape parameter* $\rho > 0$. Then, Section 4 presents an elementary numerical method to compute these standardized Voigt profiles. Finally, Section 5 applies numerical differentiation to the computed standardized Voigt profiles and establishes an empirical relationship between the location of the point of inflection and the ratio parameter ρ. This empirical relationship shows how ρ and eventually the parameters γ and σ can be read of a graph of a Voigt profile.

The relationship between the inflection point and the shape parameter allows to match Voigt profiles to line spectra directly without having to use general iterative fitting algorithms. Section 6 sketches a procedure to do so.

2 Geometries of the Gaussian and Lorentzian

Of course, the Gaussian does not need an introduction. We review only briefly the aspects relevant to our treatment of the Voigt profile.

Any Gaussian can be transformed into any other Gaussian by a linear transformation. So, the tabulated standard Gaussian is the shape prototype of all Gaussians. See Figure 1.

The transformation rule

$$G(x;\sigma/\alpha) = \frac{\alpha}{\sigma\sqrt{2\pi}} e^{-\alpha^2 x^2/(2\sigma^2)} = \alpha \cdot G(\alpha \cdot x;\sigma) \tag{4}$$

with scaling parameter $\alpha > 0$ is of particular interest. For example, for $\alpha > 1$ the expression on the right-hand side describes that the graph is compressed horizontally and stretched vertically by the factor α. The area stays the same. This has the same effect as, on the left-hand side, dividing the standard deviation σ by α, i.e. the effect of consistently compressing the width parameter. Consequently, for all Gaussians, the inflection points are invariantly one standard deviation away from the maximum. Also, the inflection points are invariantly located at the quantiles 0.1587 and 0.8413.

A Lorentzian also looks bell-shaped. See Figure 2. However, a Lorentzian approaches the horizontal asymptote $y = 0$ so slowly that the improper integrals for the expected value and the standard deviation diverge. Regardless of the symmetry about zero, the expected value and the standard deviation are undefined. We need another quantity to describe the width of a Lorentzian.

The values $\pm\gamma$ are the upper and lower quartiles. They are the locations that cut off the top and bottom 25% of the area under the Lorentzian.

As for the Gaussian we have the transformation rule

$$\begin{aligned} L(x;\gamma/\alpha) &= \frac{\gamma/\alpha}{\pi(x^2 + \gamma^2/\alpha^2)} = \frac{\gamma/\alpha}{\pi/\alpha^2\big((\alpha \cdot x)^2 + \gamma^2\big)} \\ &= \frac{\alpha\gamma}{\pi\big((\alpha \cdot x)^2 + \gamma^2\big)} = \alpha \cdot L(\alpha \cdot x;\gamma) \end{aligned}$$

for $\alpha > 0$. For example, halving the parameter γ (left-hand side), compresses the Lorentzian horizontally by the factor two and doubles it

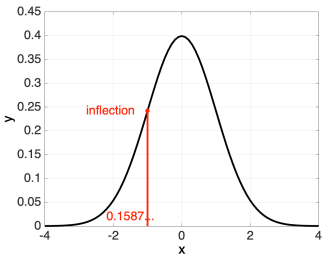

Figure 1: The Gaussian with $\sigma = 1$. The inflection points deviate are at $\pm\sigma$. The left inflection point has the quantile rank ≈ 0.1587.

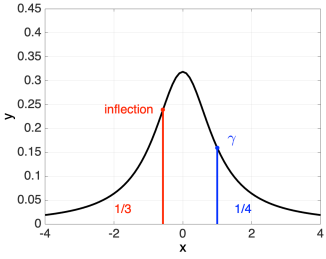

Figure 2: The Lorentzian with $\gamma = 1$. The upper and lower quartiles are at $\pm\gamma$. The left inflection point has the quantile rank $1/3$.

vertically (right-hand side). The area stays the same. The parameter γ is a sensible width parameter and has an invariant geometric meaning.

3 Standardization and Classification of Voigt Profiles

Let $\alpha > 0$. For a Voigt profile we obtain the transformation rule

$$\begin{aligned} V(x;\sigma/\alpha,\gamma/\alpha) &= \int_{-\infty}^{\infty} G(x-z;\sigma/\alpha)\, L(z;\gamma/\alpha)\, dz \\ &= \int_{-\infty}^{\infty} \alpha\cdot G(\alpha\cdot(x-z);\sigma)\, \alpha\cdot L(\alpha\cdot z;\gamma)\, dz \\ &= \int_{-\infty}^{\infty} \alpha^2\cdot G(\alpha x-\alpha z;\sigma)\, L(\alpha\cdot z;\gamma)\, dz \end{aligned}$$

Substitute $u = \alpha\cdot z$, hence $du = \alpha\, dz$,

$$\begin{aligned} &= \alpha\int_{-\infty}^{\infty} G(\alpha x-u;\sigma)\, L(u;\gamma)\, du \\ &= \alpha\cdot V(\alpha\cdot x;\sigma,\gamma) \end{aligned}$$

In particular, we get for $\alpha = \sigma$ a *standardized* expression with Gaussian width parameter 1,

$$V(x;1,\gamma/\sigma) = \sigma\cdot V(\sigma\cdot x;\sigma,\gamma) \quad . \tag{5}$$

Equivalently, every Voigt profile is a suitably scaled standardized Voigt profile,

$$V(u;\sigma,\gamma) = \frac{1}{\sigma} \cdot V\Big(\frac{u}{\sigma};1,\frac{\gamma}{\sigma}\Big) \quad . \tag{6}$$

The shape of a Voigt profile only depends on the ratio $\rho = \gamma/\sigma$. The Voigt profiles can be classified into different shapes with respect to the single parameter $\rho > 0$.

Now we show that $V(x;\sigma,\gamma)$ and $V(x;\sigma/\alpha,\gamma/\alpha) = \alpha \cdot V(\alpha \cdot x;\sigma,\gamma)$ with homogeneously scaled parameters have the inflection points at the same quantiles. Let p denote the x-coordinate of an inflection point of $f(x) = V(x;\sigma,\gamma)$, so p is a zero of the second derivative f''. The second derivative of the scaled function satisfies

$$\frac{d^2}{dx^2}\big(\alpha \cdot V(\alpha \cdot x;\sigma,\gamma)\big) = \frac{d^2}{dx^2}\big(\alpha \cdot f(\alpha \cdot x)\big) = \alpha^3 \cdot f''(\alpha \cdot x) \quad , \tag{7}$$

which possesses the correspondingly scaled zero p/α. The quantile rank at this position is given by

$$\int_{-\infty}^{p/\alpha} \alpha \cdot f(\alpha \cdot x)\, dx = \int_{-\infty}^{\alpha \cdot p/\alpha} f(u)\, du \quad , \tag{8}$$

where we substituted $u = \alpha \cdot x$ and $du = \alpha \cdot dx$. The right-hand side describes the quantile rank of the unscaled function at the inflection point p. The quantile rank of the inflection point is a scaling invariant.

Section 5 establishes empirically an increasing relationship between the shape parameter ρ and the quantile rank of the smaller inflection point. There is a one-to-one correspondence between the Voigt profile shapes and the parameter $\rho = \gamma/\sigma$.

4 Quick-and-Dirty Computation of Voigt Profiles

We compute a standardized Voigt profile $V(x;1,\rho)$ approximately by suitably truncating the improper convolution integral and by numerically integrating the remaining definite integral.

Due to the symmetry of the Gaussian, $G(x-z;\sigma) = G(z-x;\sigma)$, the Voigt profile value at x equals the integral with respect to z over the

product of the Gaussian with mean x and the centered Lorentzian.

$$\int_{-\infty}^{\infty} G(x-z;1)\, L(z;\rho)\, dz = \int_{-\infty}^{\infty} G(z-x;1)\, L(z;\rho)\, dz \tag{9}$$

We know that the values of the Gaussian are very close to zero outside $[\mu - 4\sigma, \mu + 4\sigma]$, so a sensible truncation is

$$\int_{-\infty}^{\infty} G(z-x;1)\, L(z;\rho)\, dz \approx \int_{x-4}^{x+4} G(z-x;1)\, L(z;\rho)\, dz \quad . \tag{10}$$

Since both functions, the Gaussian and the Lorentzian, can be approximated quite accurately by polynomials on reasonably small intervals, a piecewise low-degree numerical integration formula is sufficient for practical accuracy. We use the iterated trapezoid rule and iterated midpoint rule so that the proximity of the two estimates indicates how accurate they are. Moreover, the arithmetic mean of these values produces the result of the iterated trapezoid rule with twice as many subintervals. Finally, a weighted average of the two iterated trapezoid values coincides with Simpson's rule. These steps are the beginning of Romberg's scheme and can be extended, if more accuracy is needed.

To set up the iterated integration rules we divide $[x-4, x+4]$ into n equidistant subintervals of length $\Delta z = 8/n$. The trapezoid rule uses the nodes $z_k = x - 4 + k \cdot \Delta z$ with $0 \le k \le n$.

$$\begin{aligned}
V(x;1,\rho) \approx T_n(x;\rho) &= \Big(\frac{G(z_0 - x;1)\, L(z_0;\rho)}{2} + \\
&\quad \sum_{k=1}^{n-1} G(z_k - x;1)\, L(z_k;\rho) \;+\; \frac{G(z_n - x;1)\, L(z_n;\rho)}{2} \Big) \cdot \Delta z \\
&= \Big(\frac{G(-4;1)\, L(x-4;\rho)}{2} + \sum_{k=1}^{n-1} \frac{1}{\sqrt{2\pi}} e^{-(z_k - x)^2/2}\, \frac{\rho}{\pi(z_k^2 + \rho^2)} + \\
&\quad \frac{G(4;1)\, L(x+4;\rho)}{2} \Big) \cdot \frac{8}{n} \\
&= \frac{8\rho}{n\pi\sqrt{2\pi}} \cdot \Big(\frac{e^{-8}}{2\big((x-4)^2 + \rho^2\big)} + \\
&\quad \sum_{k=1}^{n-1} \frac{e^{-(-4+8k/n)^2/2}}{(x - 4 + 8k/n)^2 + \rho^2} + \frac{e^{-8}}{2\big((x+4)^2 + \rho^2\big)} \Big)
\end{aligned}$$

On the other hand, let $m_k = x - 4 + (k - 1/2)\Delta z$ with $0 \le 1 \le n$ denote the midpoints of the subintervals. The iterated midpoint rule is

$$\begin{aligned} V(x;1,\rho) \approx M_n(x;\rho) &= \sum_{k=1}^{n} G(m_k - x;1)\, L(m_k;\rho) \cdot \Delta z \\ &= \sum_{k=1}^{n} \frac{1}{\sqrt{2\pi}} e^{-(m_k - x)^2/2} \, \frac{\rho}{\pi(m_k^2 + \rho^2)} \cdot \frac{8}{n} \\ &= \frac{8\rho}{n\pi\sqrt{2\pi}} \sum_{k=1}^{n} \frac{e^{-(-4+8(k-1/2)/n)^2/2}}{(x - 4 + 8(k-1/2)/n)^2 + \rho^2} \end{aligned}$$

The trapezoid value with twice as many subintervals is the arithmetic mean

$$T_{2n}(x;\rho) = \big(T_n(x;\rho) + M_n(x;\rho)\big)/2 \tag{11}$$

and Simpson's rule is the weighted average

$$S_n(x;\rho) = \frac{4 \cdot T_{2n}(x;\rho) - T_n(x;\rho)}{3} \approx V(x;1,\rho) \quad . \tag{12}$$

Figure 3 shows some computed Voigt profiles for various ratio parameters ρ that have been computed using the above formulas with $n = 32$ subintervals at the equidistant arguments $x \in \{-16.0, -15.9, -15.8, \ldots, 16.0\}$. We use equidistant arguments to prepare for the consistent use of a finite-difference formula to determine numerically the second derivative of the Voigt profile.

5 Empirical Relationship between the Shape Parameter and the Points of Inflection

To approximate the second derivative of a Voigt profile based on the equidistant samples we use the finite difference formula

$$\frac{d^2}{dx^2} V(x;1,\rho) \approx \frac{V(x-h;1,\rho) - 2V(x;1,\rho) + V(x+h;1,\rho)}{h^2} \quad . \tag{13}$$

Figure 4 shows the second derivatives of Voigt profiles for various parameters ρ that are computed by the finite difference formula. We

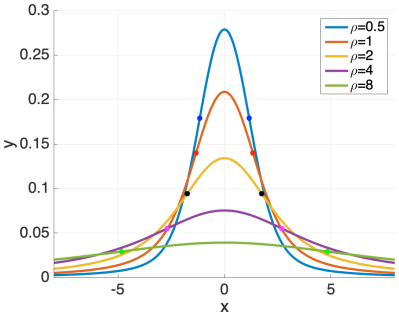

Figure 3: The standardized Voigt profiles $V(x;1,\rho)$ for various $\rho = \gamma/\sigma$ ratios and their numerically determined inflection points.

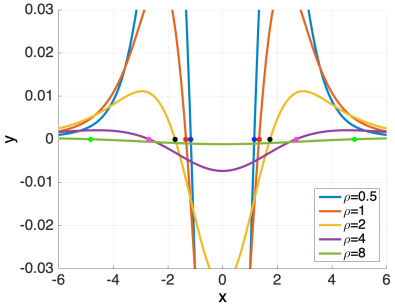

Figure 4: The numerically determined second derivatives of $V(x;1,\rho)$ for various ρ. The zeros (inflection points of V) depend monotonically on the shape-parameter.

Table 1: The positions of the inflection points for various shape parameters ρ. The limiting quantile rank for $\rho \to \infty$ seems to be $1/3$, see Figure 2.

Index ν	Shape Param. ρ_ν	Inflection Points	Quantile Rank Q_ν
Gauss	0	$(\pm 1, 0.242)$	0.1587
1	0.5	$(\pm 1.16, 0.179)$	0.2190
2	1	$(\pm 1.34, 0.140)$	0.2550
3	2	$(\pm 1.74, 0.094)$	0.2922
4	4	$(\pm 2.69, 0.055)$	0.3178
5	8	$(\pm 4.83, 0.029)$	0.3288
6	16	$(\pm 9.35, 0.015)$	0.3321
7	32	$(\pm 18.53, 0.007)$	0.3330
Lorentz	∞	n.a.	1/3

see qualitatively that the deviation of the inflection points from the mean increases with the parameter ρ. We compute estimates of these positions by finding the pair of neighboring second-derivative values with a sign change to which we apply linear interpolation. The function value estimates of the inflection points are also computed as linear interpolations of the neighboring already computed function values. The results are documented in Table 1.

According to the scatter plot in Figure 5 we start with the linear

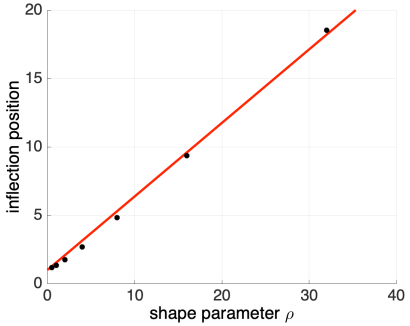

Figure 5: The location of the points of inflection depends monotonically on the shape-parameter ρ. A linear fit with theoretically prescribed intercept 1 provides a reasonable fit.

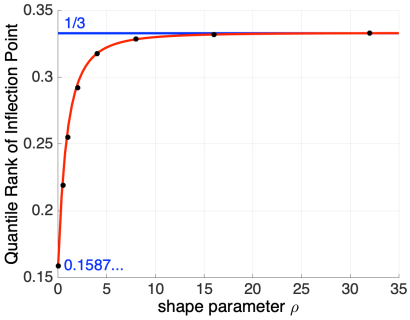

Figure 6: Relationship between quantiles of the smaller point of inflection and the shape parameter. The shown function is given by $QR = 1/3 - 1/(\rho + C)^{2.3}$ with $C = (1/3 - 0.1587)^{-1/2.3}$.

model

$$x = 1 + m \cdot \rho \quad , \tag{14}$$

in which we choose the intercept 1 from the limiting case as the position of the inflection point of the Gaussian. Based on a least squares approximation for the data points (ρ_ν, x_ν), $1 \leq \nu \leq n$, we compute the slope estimate

$$\hat{m} = \frac{\sum_{\nu=1}^{n} \rho_\nu (x_\nu - 1)}{\sum_{\nu=1}^{n} \rho_\nu^2} \approx 0.536 \; . \tag{15}$$

There is another useful relationship. We pair the shape parameter ρ with the quantile rank of the left inflection point. We have already computed estimates of the symmetrically located points of inflection. Now we numerically integrate the Voigt profile between the inflection points, subtract this estimated area from one, and divide it by half to obtain the quantile. The numerical integration uses the iterated Simpson rule on the equidistant nodes between the inflection points and, separately, computes the trapezoids from the inflection points to the neighboring node inside. The widths of these trapezoid are smaller than the

equidistant stepsize since we estimated the position (and the value) of the inflection point by linear interpolation. The resulting quantiles are listed in Tab 1 and the relationship is shown in Figure 6. By inspired guessing we have found

$$QR \approx \frac{1}{3} - \frac{1}{(\rho + C)^k} \quad \text{with } C = (1/3 - 0.1587)^{-1/k} \text{ and } k \approx 2.3\,. \tag{16}$$

6 Application to Line Spectra

To analyze a line spectrum of Voigt profiles we propose the following procedure. First, numerically compute the first and second derivatives of the spectral data. A spectral line consists of a subinterval $[\ell, m]$ with positive first derivative and a subinterval $[m, r]$ with negative first derivative. Integrate the original data over $[\ell, r]$, keeping track of the integral values from ℓ to (1) the first sign change of the second derivative, (2) the sign change of the first derivative at m, (3) the second sign change of the second derivative, and (4) the right endpoint r. Use asymmetries such as "the value at (4) is not twice the value at (2)" or "the values at (1) and (3) are not symmetric about (2)" to determine overlapping spectral lines and suitably adjust the values. The adjusted ratio (1)/(4) determines the shape parameter, the adjusted horizontal difference between the location of the maximum and the inflection points determines the parameter σ, and, finally, the adjusted value (4) determines the required vertical scaling of the Voigt profile.

The details of this procedure, especially the necessary adjustments for significantly overlapping spectral lines are the subject of current research.

References

1. W. J. Thompson, "Numerous neat algorithms for the voigt profile function," *Computers in Physics*, vol. 7, no. 6, pp. 627–631, 1993.
2. J. Wuttke and S. G. Johnson, "libcerf, numeric library for complex error functions," https://apps.jcns.fz-juelich.de/man/voigt.html, [Accessed: 2022-12-17].